Ultrasonics 69 (2016) 215–223

Contents lists available at ScienceDirect

Ultrasonics

journal homepage: www.elsevier.com/locate/ultras

Ultrasonic propagation in finite-length granular chains

D.A. Hutchins [a,*], J. Yang [a], O. Akanji [a], P.J. Thomas [a], L.A.J. Davis [a], S. Freear [b], S. Harput [b], N. Saffari [c], P. Gelat [c]

[a] School of Engineering, University of Warwick, CV4 7AL, UK
[b] School of Electronic and Electrical Engineering, University of Leeds, Leeds LS2 9JT, UK
[c] Department of Mechanical Engineering, University College London, Torrington Place, London WC1E 7JE, UK

ARTICLE INFO

Article history:
Received 26 August 2015
Accepted 19 October 2015
Available online 2 November 2015

ABSTRACT

A narrowband ultrasound source has been used to generate solitary wave impulses in finite-length chains of spheres. Once the input signal is of sufficient amplitude, both harmonics and sub-harmonics of the input frequency can be generated as non-linear normal modes of the system, allowing a train of impulses to be established from a sinusoidal input. The characteristics of the response have been studied as a function of the physical properties of the chain, the input waveform and the level of static pre-compression. The results agree with the predictions of a theoretical model, based on a set of discrete dynamic equations for the spheres for finite-length chains. Impulses are only created for very small pre-compression forces of the order of 0.01 N, where strongly non-linear behaviour is expected.

1. Introduction

The motivation for this study was the need for high amplitude, wide bandwidth ultrasonic impulses for biomedical applications. High amplitudes can be derived from ultrasonic horns, but these are of narrow bandwidth. Granular chains could, in principle, increase the available bandwidth, due to the strongly non-linear Hertzian interaction between neighbouring particles [1]. The dynamic response of these systems to impulsive input signals is governed by nonlinear, dispersive and dissipative effects, leading to the formation of solitary waves that travel along the chains [2–4]. Nesterenko has shown that characteristic solitary waves are predicted in an analytical solution using the long wave approximation [1,5]. Strongly nonlinear waves have also been observed in a chain of Teflon beads [6] and in double power-law materials [7], as well as in granular dimer chains [8].

The tunability of solitary wave properties has been demonstrated [9]. It is now known that the speed of solitary waves along a chain can be changed using an applied pre-compression force, provided the conditions of the chain are appropriate. This latter effect was used to demonstrate that a nonlinear acoustic lens with a tuneable focus can be produced [10], leading to the interesting concept of sound bullets. These sound bullets are established from an appropriate superposition of the individual output signals from a set of neighbouring Hertzian chains. These previous studies [9–11] demonstrated that piezoelectric actuation could be used to generate solitary waves in columnar chains of steel ball-bearings under small pre-compression (F_0). The resultant effects are dependent on the characteristics of the applied transient force (F_m), the diameter of the spheres, and the relative values of F_m and F_0. If $F_m \approx F_0$, weakly non-linear behaviour results, whereas if $F_m \gg F_0$, propagation along the chain is highly non-linear.

Most of the experimental work to date has used relatively low ultrasonic frequencies and large spheres with diameters of the order of up to 10 mm. The cut-off frequency for solitary waves limits the upper frequency that can propagate in chains [1]; hence, higher frequencies will need smaller spheres. In addition, little work seems to have been performed experimentally into establishing whether higher frequencies and non-impulsive waveforms could be used in chains of finite length. Of particular interest in this context is the establishment of resonances within such chains. Various papers have described the concept of Non-linear Normal Modes (NNMs) of vibration, which are expected to exist in such systems [12–14]. Jayaprakash et al. [12] studied such chains with fixed boundary conditions, and predicted a set of NNMs which resemble a traveling wave propagating backwards and forwards through the finite granular chain. These exist within allowed frequency bands (known as propagation bands), which have been observed in a two-sphere experimental system [14]. NNMs are expected to be very sensitive to the input conditions, in terms of the nature of F_m and F_0, the types of spheres used and the boundary conditions. Recent work by the current authors has investigated finite-length chains using ultrasound of a higher frequency and smaller spheres [15]. It was observed that for a given input

* Corresponding author.

http://dx.doi.org/10.1016/j.ultras.2015.10.018
0041-624X/

frequency, impulses evolved once the input amplitude exceeded a specified threshold value for a certain length chain. The present paper explores this process in much greater detail, and investigates the factors which govern the creation of these impulses. Discrete dynamic equations of motion for chains of spherical oscillators are also used to predict the signal development and propagation in such chains, for comparison to the corresponding experimental results.

2. Apparatus and experiment

The experimental arrangement used is shown in Fig. 1. Chains consisting of 1 mm diameter chrome-steel spheres, with lengths varying between 2 and 14 spheres, were placed within cylindrical holders fabricated from acrylic resin. The holders were manufactured individually from acrylic resin to suit each length of chain, using micro-stereolithography (a form of additive manufacturing). The spheres were placed horizontally within the holder so as to just touch each other, minimising the initial static pre-compression force (F_0). The first sphere was excited harmonically by a longitudinal ultrasonic horn, operating at 73 kHz, which was driven by a high voltage tone-burst signal using an Agilent 33120A function/Arbitrary waveform generator and a power amplifier. Both the horn and the chains of spheres were clamped rigidly onto an optical translation stage, and a micrometer used to position the horn against the first sphere with as little force as possible. The last sphere in the chain was held in place using an annular aperture, allowing detection of the particle velocity waveform at the output via a Polytec laser vibrometry system. The tone-burst duration and amplitude of the drive voltage signal could both be adjusted. The ultrasonic motion of the horn tip at full power, for drive voltage tone-bursts of 20 cycles and 45 cycles in duration, is shown in terms of its waveform and frequency spectrum in Fig. 2(a) and (b) respectively. Both show a prominent peak at 73 kHz, with only a small amount of harmonic content from the vibration of the horn.

3. Discrete theoretical modelling of wave propagation in chains

Here we model the acoustic wave transmission in a granular medium of finite length, contained between the ultrasonic horn and a reflecting wall, so as to understand the relationship between the input and output signals and the chain structure. This analysis also has to consider the boundary conditions at either end of the chain, as these have an effect on the resulting behaviour in a resonant system. The theoretical analysis also allows prediction of the effects resulting from changes in the static pre-compression force F_0.

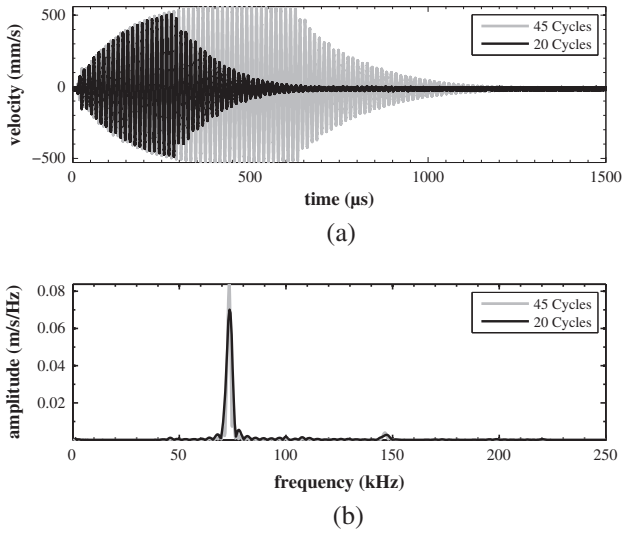

Fig. 2. (a) Waveforms and (b) spectra at the horn tip at maximum power when driven by voltage tone-bursts with durations of 20 and 45 cycles.

The discrete dynamic equations of motion [15] that describe the types of granular chains studied here assume that the spheres have an identical mass (m) and radius (R). The first sphere is harmonically excited by an ultrasonic transducer with a displacement that can be calculated from the particle velocity waveform measured experimentally at the horn tip (see Fig. 2). The first sphere in the chain is in contact with the planar face of the horn; the last sphere is assumed to be in contact with a fixed planar wall (although in practice this has an opening to allow measurement of the vibration of the last sphere in the chain). The planar surfaces of these two boundaries are, in fact, modelled as spheres with very large radii.

The model predicts the displacements of the centres of consecutive spheres ($u_1, u_2, u_3, \ldots, u_N$), for a particular input displacement waveform (u_0) from the horn tip. The experimental waveforms are observed to exhibit energy loss with elapsed time; hence, a linear viscous damping coefficient (λ) is used within the dynamic equations of motion, so that energy dissipation is included. This also helps the model to become more stable, a phenomenon observed by other authors [16]. Damping is only relevant when the spheres are in contact; if this is not the case, then a

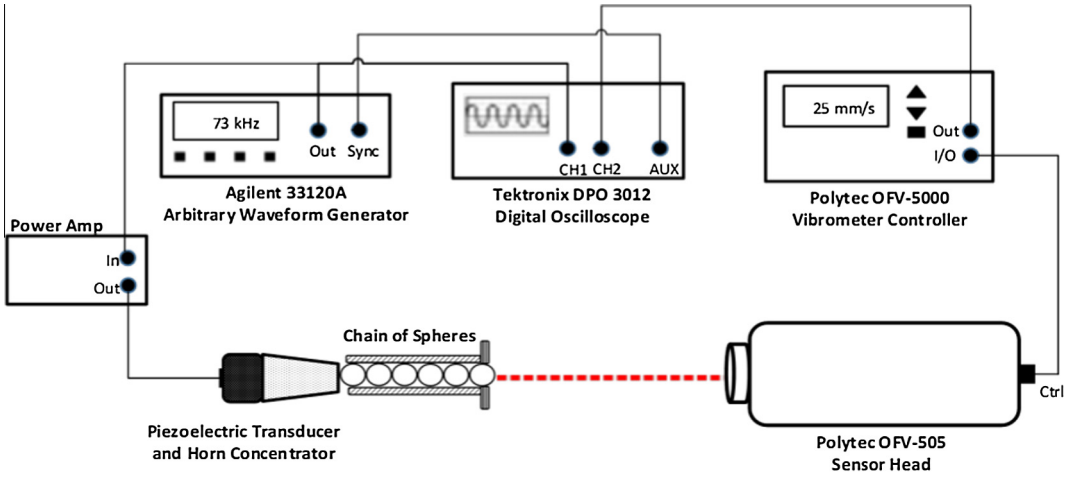

Fig. 1. Experimental arrangement used to detect signals generated by the ultrasonic horn in the chain of spheres.

damping term is not needed (as previously described by Lydon et al. [14]). This is dealt with via the Heaviside function H included within the equations. The effect of a static pre-compression force F_0 is modelled by computing an initial static displacement of the centre of each sphere in the chain from its zero-force state. This differs at the two ends of the chain from that present for intermediate spheres, because of boundary conditions. The resulting starting displacements are denoted as δ_{0l} (between the horn and the first sphere), δ_0 (between intermediate spheres), and δ_{0r} (between the last sphere and the end wall) respectively.

As will be demonstrated below, the exact conditions of the chain have to modelled carefully, as the nonlinear normal modes that are created are sensitive to this. It is thus necessary to define effective Young's moduli associated with contact interactions between the horn and the first sphere, between intermediate spheres, and between the last sphere and the end wall (θ_l, θ_m and θ_r respectively). These quantities have values which depend on the material properties of the spheres, according to

$$\frac{1}{\theta_l}=\frac{1-\nu_l^2}{E_l}+\frac{1-\nu_s^2}{E_s}\quad \theta_m=\frac{E_s}{1-\nu_s^2}\quad \frac{1}{\theta_r}=\frac{1-\nu_r^2}{E_r}+\frac{1-\nu_s^2}{E_s}, \tag{1}$$

where E_l and ν_l are the Young's modulus and Poisson ratio of the horn, E_r and ν_r are that of the far end wall, and E_s and ν_s those of the spheres themselves. The values of δ_{0l}, δ_0 and δ_{0r} are then given by

$$\delta_{0l}=\left(\frac{3F_0}{4\sqrt{R}\theta_l}\right)^{2/3}\quad \delta_0=\left(\frac{3F_0}{\sqrt{2R}\theta_m}\right)^{2/3}\quad \delta_{0r}=\left(\frac{3F_0}{4\sqrt{R}\theta_r}\right)^{2/3}. \tag{2}$$

For the input sphere next to the horn, the equation of motion in terms of particle displacement in a chain containing N spheres is [15]:

$$\begin{aligned} m\frac{d^2u_1}{dt^2}=&\frac{2\sqrt{R}}{3}\left[2\theta_l(\delta_{0l}+u_0-u_1)^{3/2}-\frac{\theta_m}{\sqrt{2}}(\delta_0+u_1-u_2)^{3/2}\right]\\ &+\lambda\left(\frac{du_0}{dt}-\frac{du_1}{dt}\right)H(\delta_{0l}+u_0-u_1)\\ &-\lambda\left(\frac{du_1}{dt}-\frac{du_2}{dt}\right)H(\delta_0+u_1-u_2). \end{aligned} \tag{3}$$

For intermediate spheres in the chain, the relevant equation of motion is:

$$\begin{aligned} m\frac{d^2u_i}{dt^2}=&\frac{\sqrt{2R}}{3}\theta_m[(\delta_0+u_{i-1}-u_i)^{3/2}-(\delta_0+u_i-u_{i+1})^{3/2}]\\ &+\lambda\left(\frac{du_{i-1}}{dt}-\frac{du_i}{dt}\right)H(\delta_0+u_{i-1}-u_i)\\ &-\lambda\left(\frac{du_i}{dt}-\frac{du_{i+1}}{dt}\right)H(\delta_0+u_i-u_{i+1}). \end{aligned} \tag{4}$$

At the far end of the chain, the equation becomes

$$\begin{aligned} m\frac{d^2u_N}{dt^2}=&\frac{2\sqrt{R}}{3}\left[\frac{\theta_m}{\sqrt{2}}(\delta_0+u_{N-1}-u_N)^{3/2}-2\theta_r(\delta_{0r}+u_N)^{3/2}\right]\\ &+\lambda\left(\frac{du_{N-1}}{dt}-\frac{du_N}{dt}\right)H(\delta_0+u_{N-1}-u_N)-\lambda\frac{du_N}{dt}H(\delta_{0r}+u_N). \end{aligned} \tag{5}$$

Note that negative values of the force terms involving successive spheres in Eqs. (3)–(5) imply that the relevant two neighbouring spheres have lost contact and the terms are then set equal to zero; additionally the damping term involving the Heaviside function H then becomes inactive, as explained above.

For comparison to the present experiments, numerical solutions of these equations were obtained using a technique developed for molecular dynamics, namely the Velocity Verlet method. This method has been used, for example, in the simulation of the dynamics of particles in suspensions [16]. It is particularly suited to discrete systems, such as the present situation involving the study of the motion of individual spheres. The relevant material parameters required for the calculations are given in Table 1. The value of λ required to get good agreement with experiment increased with the length of each chain, due to increased dissipation, over the range $\lambda = 0.23$–0.32 N s m^{-1} from 3 to 10 spheres in length. This damping is thought to arise primarily from dissipation caused by contact of spheres with the viscoeleastic polymer holder used to contain the spheres.

4. Experimental results and comparison to theory

Here, we report details of the experimental results, including the dependence of propagation along the chain on the input waveform characteristics. This has been performed for a series of chain configurations, in terms of chain length, sphere size, sphere material and end-wall conditions. Additional comparisons of experimental results to theoretical predictions allow a more in-depth analysis of the behaviour of the chains to be performed.

4.1. A chain of 6 steel spheres of 1 mm diameter

Experiments were performed initially on a chain of six chrome-steel spheres, and particle velocity waveforms recorded at the last sphere in the chain as the input was varied in terms of tone-burst duration and amplitude. Note that the vibrometer was also used to record the input signal from the horn tip in all experiments, so that the correct input waveform could be used for theoretical predictions to compare with a given experiment. These experiments were all performed using the minimum static pre-compression force (F_0) achievable in the apparatus of Fig. 1, with the horn just touching the first sphere. Comparisons between computations and experiments, to be discussed further below, revealed that the magnitude of this force is of the order of 0.01 N.

It was found experimentally that the output signal at the far end of the chain was highly dependent upon the characteristics of the input waveform, in terms of both amplitude and duration of the input signal at 73 kHz. Consider first the use of a 20-cycle voltage excitation signal into the horn (see Fig. 2 for the input velocity waveform from the horn at maximum power). Fig. 3 shows the results obtained for a 6-sphere chain as the input amplitude was gradually increased up to this maximum. Here we use v_m to represent the maximum pk–pk amplitude of the input velocity waveform for each measurement. At low amplitudes of the input ($v_m = 87$ mm s^{-1}), the output signal at the far end of the chain was small, with characteristics that were mainly those of the drive signal, although a small increase in the harmonic at 146 kHz indicated some limited non-linearity. As the input signal was then increased in amplitude, the time waveform started to change so as to incorporate a second feature with a period different to that of the input signal. This was associated with the appearance of additional regularly-spaced peaks in the frequency spectrum, at both higher and lower frequencies than the input at 73 kHz. As the magnitude of the input signal increased further, the new periodicity in the time waveform became more obvious, so that at the highest input amplitude, a set of distinct regularly-spaced impulses can be seen in the time waveform. This was associated

Table 1
Material constants used in the theoretical model.

Material	Young's modulus (GPa)	Poisson's ratio
Ultrasonic horn (steel)	$E_l = 201$	$\nu_l = 0.3$
Spheres (steel)	$E_s = 201$	$\nu_s = 0.3$
End wall (acrylic polymer)	$E_r = 2.45$	$\nu_r = 0.35$

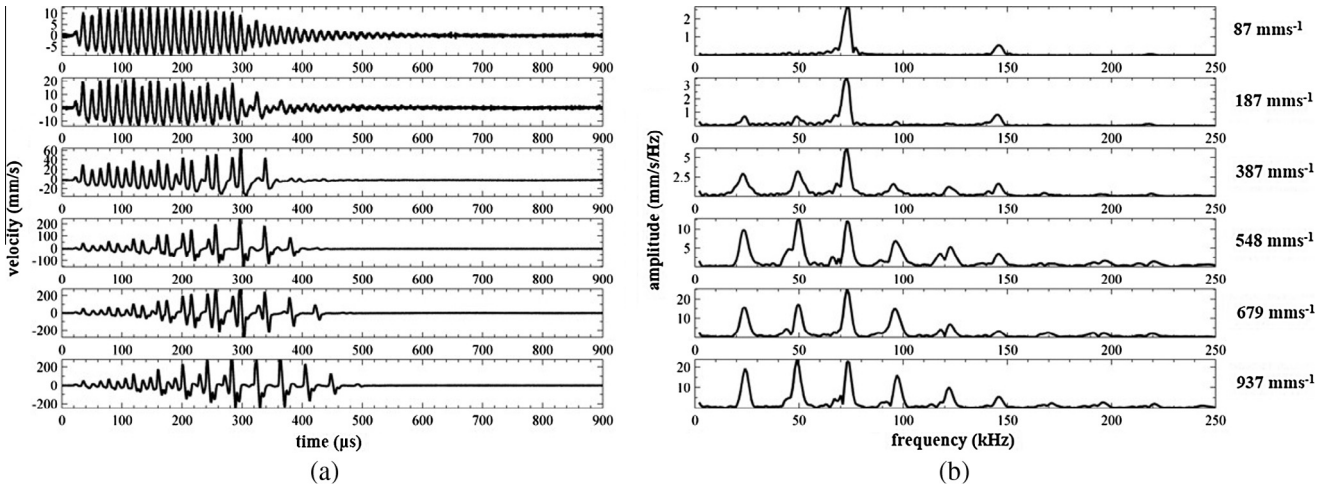

Fig. 3. (a) Waveforms and (b) frequency spectra of signals recorded at the output of a 6-sphere chain as the input amplitude was increased. The input was in the form of a tone-burst from the ultrasonic horn at 73 kHz, such as that shown in Fig. 2(a). The maximum pk–pk input amplitude (v_m) is given on the right in each case.

with an increase in the prominence of the set of regularly-spaced peaks in the frequency spectrum. It is interesting to note that these frequency peaks were spaced at a value of 1/3 of that of the excitation frequency. They thus represent a set of two sub-harmonics, plus a set of harmonics, generated as a result of propagation along the chain. All the main frequency peaks are integer multiples of the lowest peak in the spectrum at 24.3 kHz. The periodicity of impulses in the time waveform was 41 μs, the reciprocal of this value. Note that at the higher input amplitudes ($v_m = 937$ mm s^{-1}), the two sub-harmonic peaks were of higher amplitude than any of the harmonics. This generation of distinct sub-harmonics is observed in our experiments to be a characteristic feature of such systems in situations where impulses appear in the time-domain waveform.

The experimental results shown in Fig. 3 can be compared to the predictions of theory, so as to gain greater insight into the processes at work. As stated above, the experimental arrangement is assumed to impose a small pre-compression force (F_0) onto the chain. At low input amplitudes ($v_m = 87$ mm s^{-1}), a weakly non-linear behaviour is exhibited in the experiment, with the enhancement of the first harmonic, indicating the presence of such a small pre-compression force. Such behaviour was also observed in the work of Lydon et al. [14] in their study of a two-sphere system. They indicated that experimental and numerical results did not agree quantitatively in the nominally zero pre-compression state; they then went on to analyse the situation more closely, and identified a small unintended pre-compression as the cause. In the present case, the addition of a small pre-compression force $F_0 = 0.012$ N was seen to produce good agreement between theory and experiment. The predicted waveform of Fig. 4 is now similar to that measured experimentally, in that the predicted signal is predominantly that of the input, modified by the addition of some harmonic content in the frequency spectrum. Hence a pre-compression force of this magnitude was thus assumed to exist in the modelling predictions to follow.

The predicted waveform and corresponding frequency spectrum for an intermediate input amplitude of $v_m = 378$ mm s^{-1} (Fig. 5 (top)) contain features that agree with those seen experi-

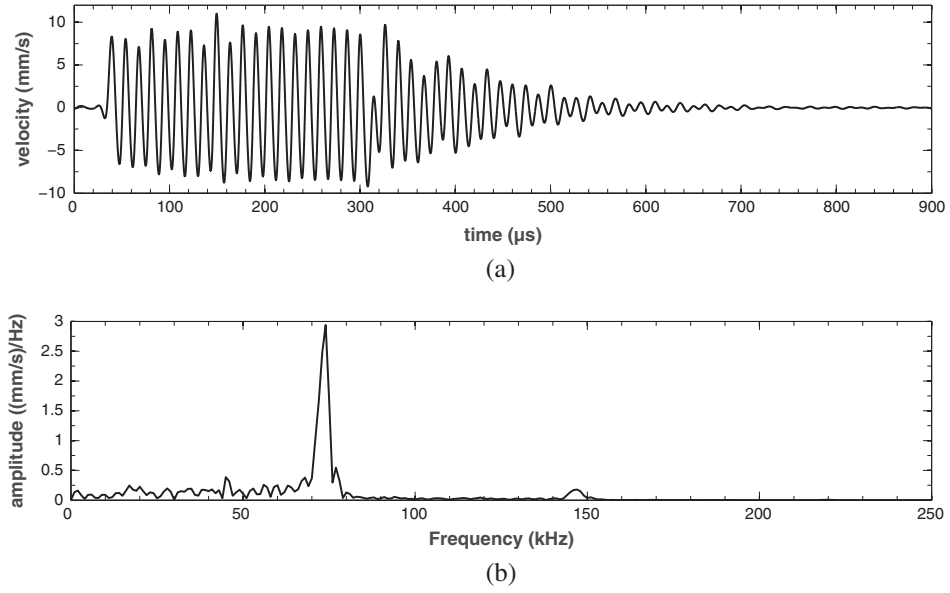

Fig. 4. Modelling results for the output signal from a 6-sphere chain, assuming a small input amplitude of $v_m = 87$ mm s^{-1} from the ultrasonic horn, for a pre-compression force of $F_0 = 0.012$ N. (a) The predicted time waveform and (b) the corresponding frequency spectra.

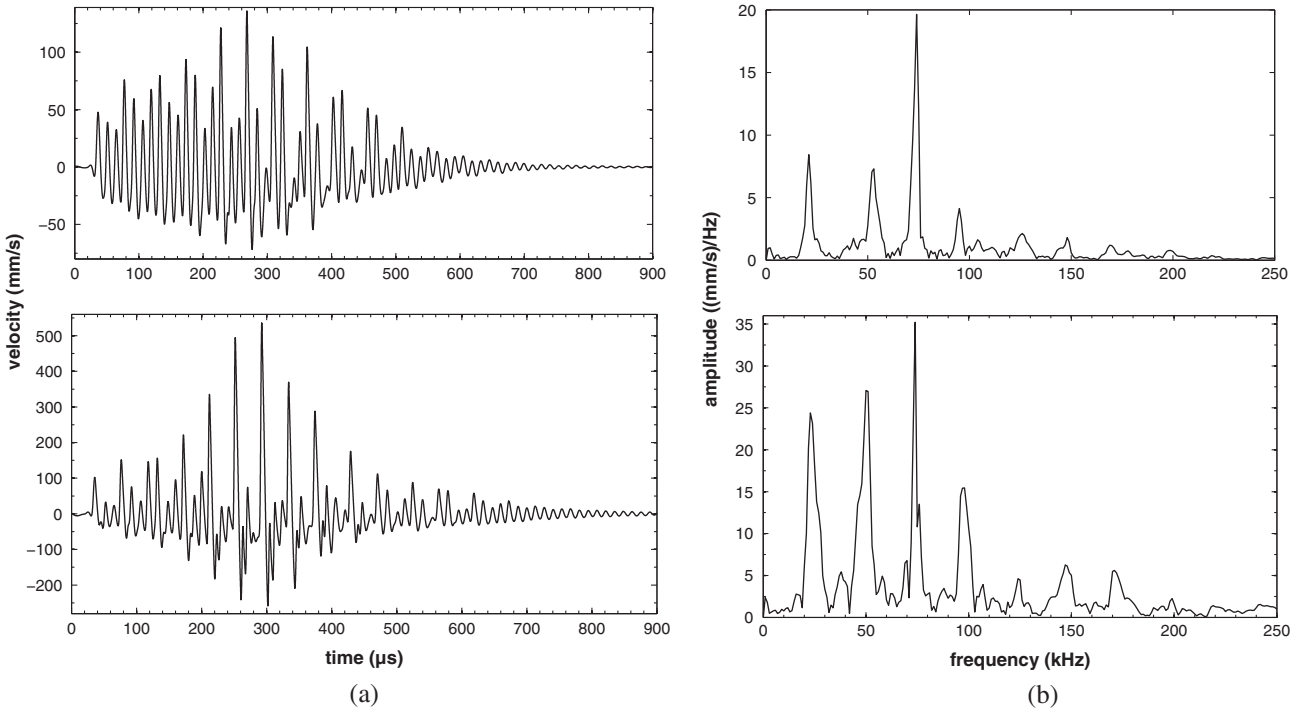

Fig. 5. Modelling predictions for a 6-sphere chain for both an intermediate amplitude of $v_m = 378$ mm s^{-1} (top) and at the maximum input amplitude of $v_m = 937$ mm s^{-1} (bottom). (a) The predicted time waveform and (b) the corresponding frequency spectrum in each case.

mentally, namely a form of transitional behaviour between the weakly nonlinear signals and the strong solitary wave pulses. Fig. 5 also shows predictions for the highest input amplitude ($v_m = 937$ mm s^{-1}), where the predicted motion at the end of the chain is a set of impulses with strong sub-harmonics in the spectrum, and has the main features seen in the experimental waveform of Fig. 3 at the highest input amplitude. The correct frequency components are predicted, as are the periodicity and general nature of the impulses in the time domain. There are minor differences in the magnitude of the frequency peaks between theory and experiment, but overall the agreement is very good.

Experimentally, there was also a dependence on the number of cycles in the excitation waveform, as is demonstrated in Fig. 6 for 10, 20 and 30-cycle excitations. At 10 cycles, the impulses were not fully formed, and the spectral peaks were indistinct. The optimum result in terms of the creation of impulses occurred at 20 cycles. At longer inputs of 30 cycles, the amplitudes of both harmonics and sub-harmonics decreased relative to the main input frequency of 73 kHz, and the impulses became less distinct. This process continued for longer input signals. Note also that the measured pk–pk amplitude increased with longer excitation waveforms, a consequence of the additional energy being input into the spherical chain.

4.2. Results for different chain lengths of 1 mm diameter steel spheres

The above experiments were repeated for different chain lengths, ranging from 2 to 10 spheres. As in the case for 6 spheres, the output was a function of both the amplitude and the number of cycles in the waveform. The results for a 10-sphere chain of 1 mm diameter steel spheres are shown in Fig. 7, again as a function of input amplitude. It was found that the optimum result in terms

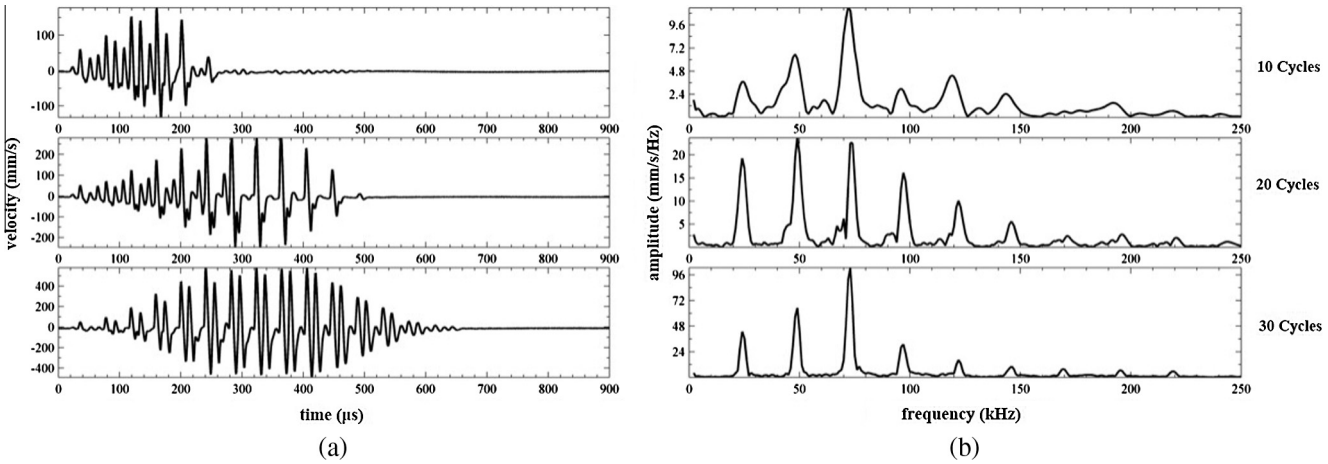

Fig. 6. Experimental waveforms showing the effect of changing the number of cycles (given on the right) in the drive waveform for a 6-sphere chain, at the maximum input amplitude of $v_m = 937$ mm s^{-1}. (a) Time waveform and (b) corresponding frequency spectrum.

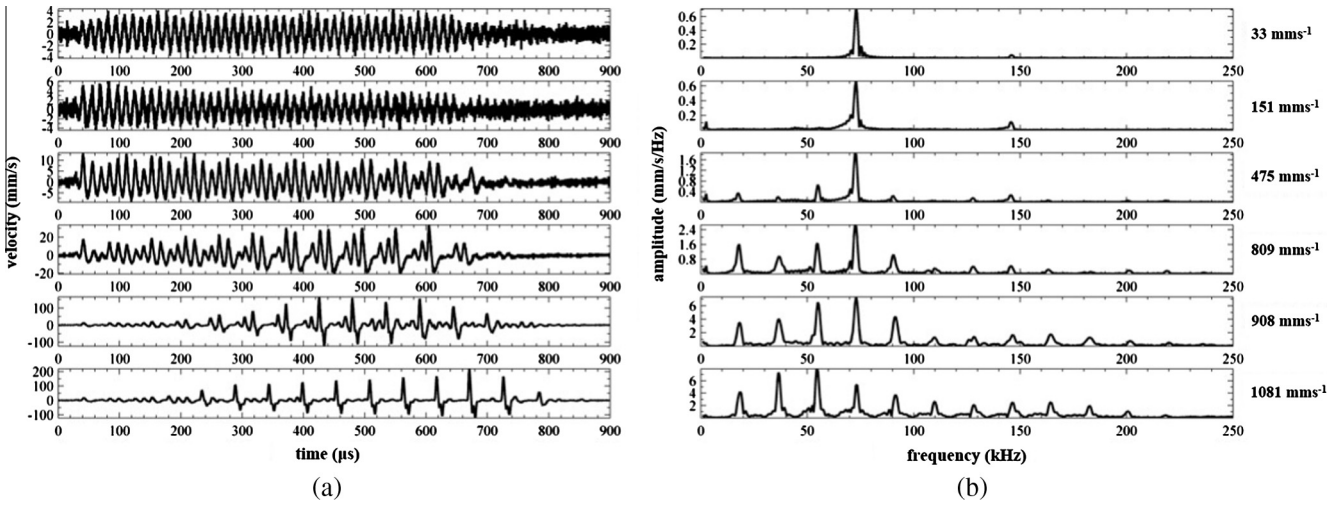

Fig. 7. (a) Waveforms and (b) frequency spectra of output signals recorded for a 10-sphere chain, using a 45-cycle tone-burst from the ultrasonic horn at 73 kHz (Fig. 2(a)). The maximum pk–pk input amplitude v_m is given on the right in each case.

of impulse formation for a 10-sphere chain occurred when the tone-burst excitation waveform was increased to be 45 cycles in length (an example was shown earlier in Fig. 2). In this case, the impulses were fully formed at the maximum input amplitude, and were seen to exist over a longer time duration than in the 6-sphere case, before again decaying away once the excitation was removed. Note that the input frequency of 73 kHz was a prominent peak for both chain lengths of 6 and 10 spheres, as would be expected. However, now the frequency spectrum of the longer chain contained three sub-harmonics, instead of the two seen for the 6-sphere case, and the lowest frequency peak was at a lower frequency of 18.25 kHz (*i.e.* 1/4 that of the input). The corresponding time between impulses was 54.8 μs. Note that this change in time separation between impulses is not in direct proportion to chain length, when a comparison is made to the 6-sphere case. This is not unexpected for such a highly-nonlinear system. It is also evident that the longer chain length has resulted in a wider bandwidth at the maximum input signal level, with sharper peaks in the time waveform, and an extended spectrum.

Modelling confirms the expected behaviour for this longer chain. The predictions are shown in Fig. 8 for the 45-cycle input at maximum amplitude. Again, the main features of the experimental waveform and spectrum are predicted – distinct impulses are predicted at the correct spacing in time, with the spectrum containing peaks separated by a value 1/4 that of the input frequency. Prominent sub-harmonics are present, as expected.

Comparison of the results for the two lengths of chain indicates some interesting features. The time-domain train of impulses has a regular periodicity in each case, but with a longer period for the longer chain. This is associated with a smaller separation of the equivalent regular frequency peaks in the frequency spectrum. In addition, all of the main peaks are multiples of the lowest frequency peak (1/3 and 1/4 of 73 kHz for the 6 and 10 sphere chains respectively). These represent some of the allowed NNMs of the

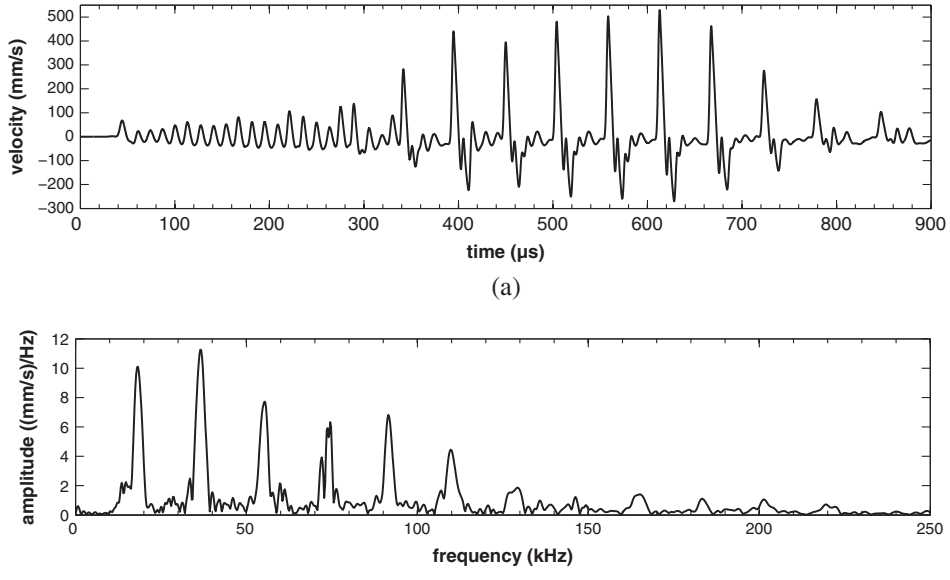

Fig. 8. Modelling results for a 10-sphere chain, assuming the 45-cycle time waveform of Fig. 2(b) as the input at the highest input amplitude from the horn at v_m = 1081 - ms^{-1}(Fig. 2(b)). (a) Time waveform and (b) frequency spectrum.

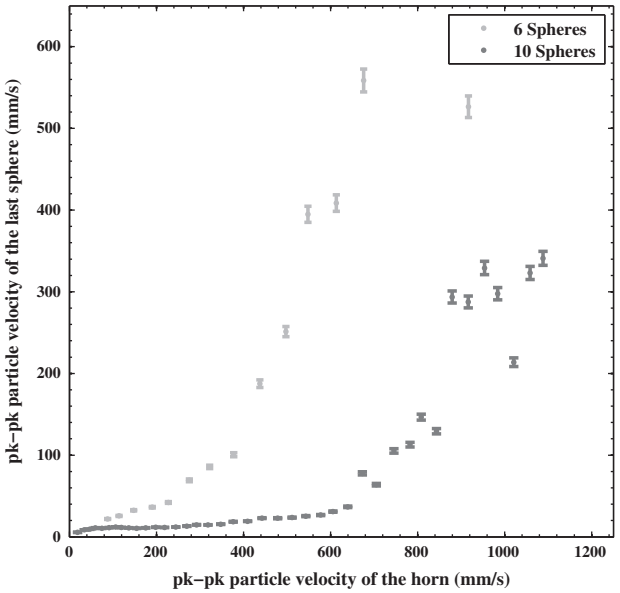

Fig. 9. Dependence of output pk–pk maximum amplitude on that of the input, as measured by the vibrometer in chains containing both 6 and 10 spheres.

chain. The first peak in each case represents the lowest-frequency NNM resonance permitted as a whole fraction (*i.e.* a sub-harmonic) of the input frequency for that chain length. This reciprocal of this frequency corresponds to the time interval between impulses in each time waveform. Both harmonics and sub-harmonics are generated, as they are all allowed resonances of the chain. Note that the input drive waveform will contain some energy at all frequencies in this spectrum, due to its finite time duration, even though this may be very small; hence, sub-harmonics can grow from this small seed energy level.

Experimentally, it is observed that the increase in the maximum pk–pk amplitude of the particle velocity measured at the output is not a linear function of the input amplitude. This is illustrated in Fig. 9 for chains containing 6 and 10 spheres. Initially, the output is approximately proportional to the input levels. However, at a certain point, the amplitudes grow more quickly, before reaching a saturation level, after which the amplitude appears to vary erratically. This behaviour is not dissimilar to that expected from finite-amplitude resonant systems in which sub-harmonic generation is involved, such as those seen in bubble dynamics [17,18].

The result obtained experimentally for a 3-sphere chain of 1 mm diameter spheres is shown in Fig. 10 (top). As might be expected, it falls within the pattern observed thus far – now there is only one sub-harmonic, at 1/2 the frequency of the input, with the corresponding repetition rate of the time-domain impulses being the reciprocal of this value. There is also only one distinct harmonic. The trends observed for the chains containing 6 and 10 spheres have thus continued – for the creation of impulses, a whole fraction of the input frequency needs to be present as the lowest peak in the spectrum, and all other significant peaks are multiples of this. In addition, the apparent propagation velocity of impulses within the chain decreases as the chain gets shorter.

Experiments have been performed for all chain lengths in the 2–14 range. The effects of resonance and the generation of a train of impulses for sphere diameters of 1 mm at an excitation frequency of 73 kHz were only observed in the case of 3, 6 and 10 spheres. This was irrespective of the amplitude or number of cycles in the input signal. This indicates that conditions were not well-matched for the creation of NNM resonances and pass-band behaviour in these chain lengths, for the size of steel spheres and input frequency used.

4.3. Use of a different sphere material

Experiments were also conducted on 1 mm diameter thermoplastic polymer spheres, in this case polyoxymethylene (Delrin™), and tungsten carbide ceramic spheres of the same size. Table 2 compares their material properties to those of acrylic polymer (used to make the holder for the spheres) and the steel ball-bearings.

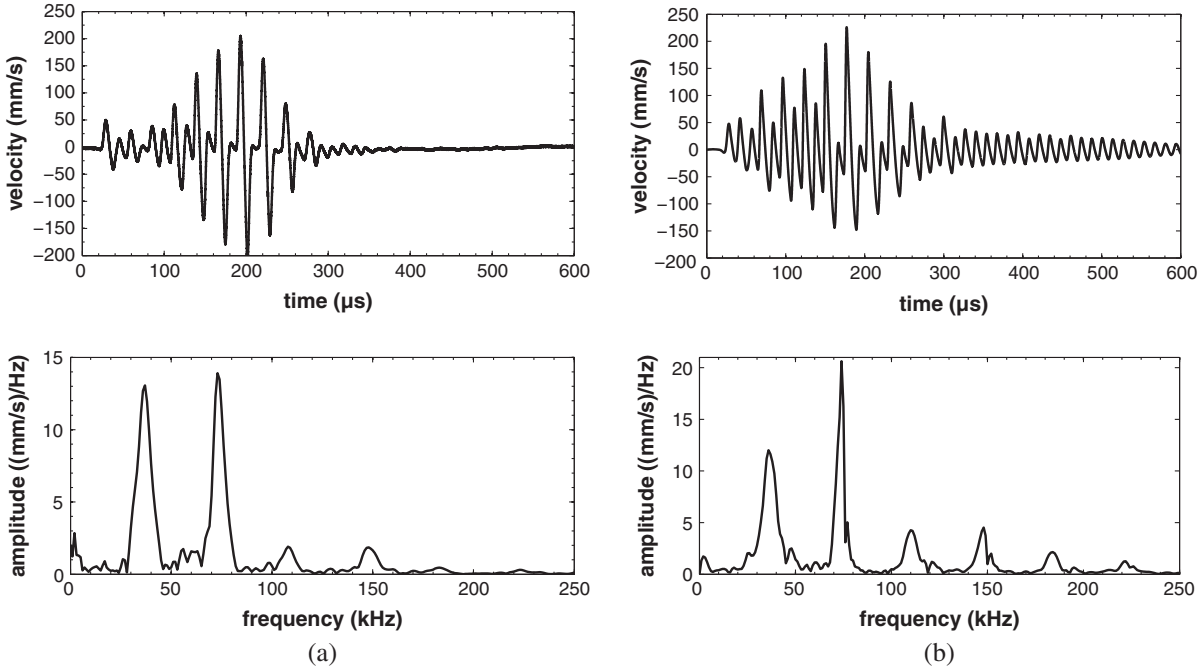

Fig. 10. Results for a 3-sphere chain of steel spheres of 1 mm diameter using an input waveform in each case of 10 cycles at 73 kHz and with $v_m = 634$ mm s^{-1}. (a) Experimental result and (b) theoretical prediction, showing waveform (top) and frequency spectrum (bottom) in each case.

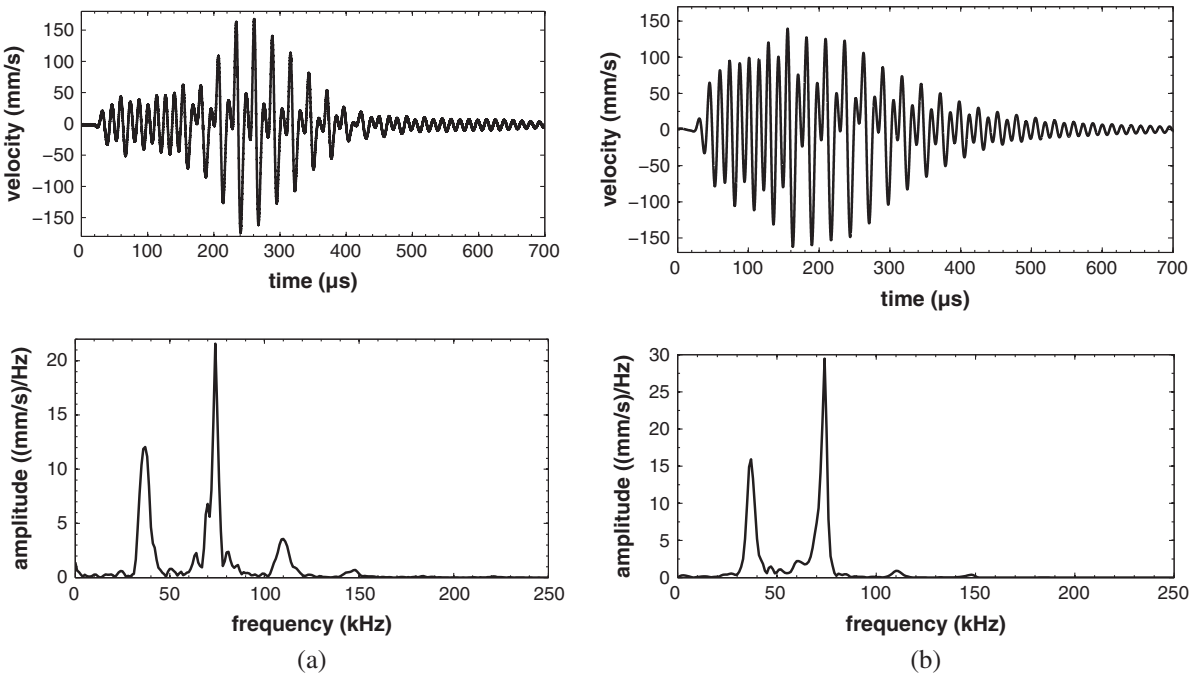

Fig. 11. Experimental result for a 3-sphere chain of Delrin spheres of 1 mm diameter, using an input waveform of 10 cycles at 73 kHz and with $v_m = 634$ mm s^{-1}. (a) Experimental result and (b) theoretical prediction, showing waveform (top) and frequency spectrum (bottom) in each case.

It can be seen that Delrin differs from steel in being reasonably well-matched in terms of the acoustic impedance vale (Z) to the acrylic polymer used for the holder end-plate. The results for a 3-sphere chain are shown in Fig. 11. In common with the results for a 3-sphere chain of steel spheres of the same size, Fig. 10, only one sub-harmonic is present, and a train of solitary-wave impulses is seen. The results for tungsten carbide (Fig. 12) indicate again that only one sub-harmonic is present, although in this case of a higher amplitude than for either steel or Delrin. These results seem to indicate that changing the sphere material is less important than changing the number of spheres in a chain in terms of determining the main frequency components present in the resultant train of solitary wave impulses.

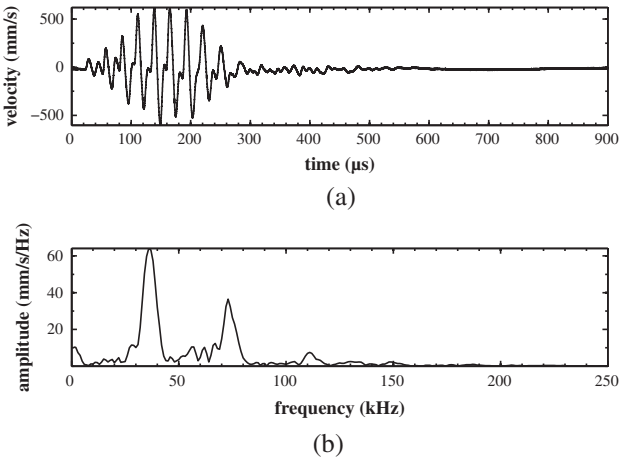

Fig. 12. Experimental result for a 3-sphere chain of tungsten carbide spheres of 1 mm diameter, using an input waveform of 10 cycles at 73 kHz and with $v_m = 634$ mm s^{-1}, showing (a) waveform and (b) frequency spectrum.

5. Discussion

The above has demonstrated that interesting effects occur when high amplitude ultrasonic sinusoidal signals are input into a resonant chain of spheres. For a situation where the pre-compression F_0 is very small, the output is highly sensitive to both the exact conditions of the chain, and small changes to the input. At high input amplitudes, strongly nonlinear behaviour is observed due to Hertzian contact between spheres. Provided the amplitude and tone-burst length of the input signal are at chosen correctly, NNM resonances can exist in the form of both harmonics and sub-harmonics of the main input frequency. The effect is to create a series of solitary-wave impulses, whose characteristics depend on the structure of the chain. This type of NNM behaviour is only observed in our experiments in a certain number of chain lengths using 1 mm chrome steel spheres, namely 3, 6 and 10 spheres in the present experiments. It is thus postulated that, as we are using a fixed input frequency and sphere material, only certain chain lengths will allow resonances in the form of NNMs to be present. Modelling studies using the dynamic equations of motion presented above confirm this behaviour. Thus, the characteristics of the chain will have to be chosen carefully if solitary wave impulses are to be generated using a specific input frequency (the latter being fixed in our experiments because of the use of a highly-resonant horn as an ultrasonic source).

The experiments have shown that the output is very dependent on the input conditions. The input has to be fine-tuned to produce time-domain impulses from the sinusoidal input; both the amplitude and number of cycles in the input waveform have to be adjusted to achieve the best results for a given spherical chain with allowed NNMs. The number of spheres present at a particular frequency has a big effect on the resultant output; however, for a fixed chain length, the material properties of the spheres seems to be of secondary importance in determining the main features present in the resultant waveforms.

Modelling the behaviour by solving discrete dynamic equations of motion for each sphere in the chain is able to predict the main features of the observed experimental results. Strongly nonlinear oscillations are predicted, involving both compression and loss of

Table 2
Material properties of three materials used in these experiments.

Material	Bulk acoustic velocity c (ms^{-1})	Density ρ ($\times 10^3$ kg m^{-3})	Acoustic impedance Z (MRayls)
Acrylic polymer	2710	1.19	3.26
Chrome steel	5900	7.83	46
Delrin polymer	2400	1.42	3.45
Tungsten carbide	6656	13.8	91.9

contact between spheres, and these are modelled within the dynamic equations. The experimental conditions meant that some level of static pre-compression force F_0 was always present; this modified the behaviour throughout, especially at low input amplitudes, where the behaviour was weakly non-linear. At low values of F_0, however, the deliberate use of narrow bandwidth inputs of high amplitude meant that resonances in the form of NNMs were encouraged, leading to prominent harmonic and sub-harmonic generation. It is the presence of multiple NNM resonances that allows the formation of impulsive signals at high amplitude. In our experiments, the output signals can reach values of 50% of that of the input (see Fig. 9). This means that the impulses themselves are of reasonably high amplitude, leading to the possibility of uses in therapeutic ultrasound.

6. Conclusions

It has been demonstrated that impulses can be generated from high amplitude, narrow bandwidth inputs into chains of steel spheres. These are only created when the experimental conditions are correctly fine-tuned, in terms of the input waveform characteristics and the applied pre-compression force for a given chain. When this is done, a set of NNMs can be excited, which form a set of harmonics and sub-harmonics of the input frequency; it is this that leads to the creation of a train of impulses, the characteristics of which depend on the chain length for a given sphere material and diameter. These effects only occur for very small pre-compression forces F_0, where strongly non-linear behaviour occurs. These results are likely to have uses in many branches of ultrasound, where the creation of high amplitude impulses is required. This includes biomedical therapeutic ultrasound, targeted drug delivery, sonochemistry and many other fields.

Acknowledgement

The authors gratefully acknowledge funding from the Engineering and Physical Sciences Research Council (UK) via grant number EP/K030159/1.

References

[1] V.F. Nesterenko, Propagation of nonlinear compression pulses in granular media, J. Appl. Mech. Tech. Phys. 24 (1983) 733–743.
[2] C. Coste, E. Falcon, S. Fauve, Solitary waves in a chain of beads under Hertz contact, Phys. Rev. E 56 (1997) 6104–6117.
[3] S. Sen, J. Hong, E. Avalos, R. Doney, Solitary waves in a granular chain, Phys. Rep. 462 (2008) 21–66.
[4] R.S. Mackay, Solitary waves in a chain of beads under Hertz contact, Phys. Lett. A 251 (1999) 191–192.
[5] V.F. Nesterenko, Dynamics of Heterogeneous Materials, Springer-Verlag, New York, 2001.
[6] C. Daraio, V.F. Nesterenko, E. Herbold, S. Jin, Strongly nonlinear waves in a chain of Teflon beads, Phys. Rev. E 72 (2005) 016603.
[7] E.B. Herbold, V.F. Nesterenko, Solitary and shock waves in discrete strongly nonlinear double power-law materials, Appl. Phys. Lett. 90 (2007) 261902.
[8] K.R. Jayaprakash, Y. Starosvetsky, A.F. Vakakis, A new family of solitary waves in granular dimmer chains with no pre-compression, Phys. Rev. E 83 (2011) 036606.
[9] C. Daraio, V.F. Nesterenko, E. Herbold, S. Jin, Tunability of solitary wave properties in one-dimensional strongly nonlinear phononic crystals, Phys. Rev. E 73 (2006) 026610.
[10] A. Spadoni, C. Daraio, Generation and control of sound bullets with a nonlinear acoustic lens, Proc. Natl. Acad. Sci. 107 (2010) 7230–7234.
[11] C.M. Donahue, P.W.J. Anzel, L. Bonanomi, T.A. Keller, C. Daraio, Experimental realization of a nonlinear acoustic lens with a tunable focus, Appl. Phys. Lett. 104 (2014) 014103.
[12] K.R. Jayaprakash, Y. Starosvetsky, A.F. Vakakis, M. Peeters, G. Kerschen, Nonlinear normal modes and band zones in granular chains with no pre-compression, Nonlinear Dyn. 63 (2011) 359–385.
[13] Y. Starosvetsky, A.F. Vakakis, Traveling waves and localized modes in one-dimensional homogeneous granular chains with no pre-compression, Phys. Rev. E 82 (2009) 026603-1–02660314.
[14] J. Lydon, K.R. Jayaprakash, D. Ngo, Y. Starosvetsky, A.F. Vakakis, C. Daraio, Frequency bands of strongly nonlinear homogeneous granular systems, Phys. Rev. E 88 (2013) 012206(9).
[15] D.A. Hutchins, J. Yang, O. Akanji, P.J. Thomas, L.A.J. Davis, S. Freear, S. Harput, N. Saffari, P. Gelat, Evolution of ultrasonic impulses in chains of spheres using resonant excitation, Eur. Phys. Lett. 109 (2015) 54002.
[16] N.S. Martys, R.D. Mountain, Velocity Verlet algorithm for dissipative-particle-dynamics-based models of suspensions, Phys. Rev. E 59 (1999) 3733–3736.
[17] A. Eller, H.G. Flynn, Generation of subharmonics of order one-half by bubbles in a sound field, J. Acoust. Soc. Am. 46 (1969) 722.
[18] S. Harput, M. Arif, J. McLaughlan, D.M.J. Cowell, S. Freear, The effect of amplitude modulation on subharmonic imaging with chirp excitation, IEEE Trans. Ultrason. Ferroelectr. Freq. Control 60 (2013) 2532–2544.